SEISMIC CALIBRATION OF GROUP 1 INTERNATIONAL MONITORING SYSTEM (IMS) STATIONS IN EASTERN ASIA FOR IMPROVED EVENT LOCATION

John R. Murphy,[1] William L. Rodi,[2] Michelle Johnson,[3] Jamil D. Sultanov,[4] Theron J. Bennett,[1]
M. Nafi Toksoz,[2] Carolynn E. Vincent,[3] Vladimir Ovtchinnikov,[4] Brian W. Barker,[1]
Anca M. Rosca,[3] and Yuri Shchukin[4]

Science Applications International Corporation,[1] Massachusetts Institute of Technology,[2]
Weston Geophysical Corporation,[3] Institute for Dynamics of the Geospheres[4]

Sponsored by Defense Threat Reduction Agency

Contract No. DTRA01-00-C-0024

ABSTRACT

A consortium of institutions that includes SAIC, Massachusetts Institute of Technology's (MIT's) Earth Resources Laboratory (ERL), Weston Geophysical Corporation and the Russian Institute for Dynamics of the Geospheres (IDG) is engaged in a research program directed toward the seismic travel-time calibration of the 30 Group 1 International Monitoring System (IMS) stations of eastern Asia. During the second year of this program, we have refined our preliminary 3-D velocity model of the region to incorporate a 1°-x-1° background model based on the surface wave inversion studies of Stevens and Adams (2001), as well as new submodels of the China, southeast Asia, and Korean peninsula regions. In addition, we have formulated and implemented a sophisticated, fully nonlinear tomographic inversion algorithm and applied it to the refinement of our velocity models of the Former Soviet Union (FSU) DSS region and the India/Pakistan region (WINPAK3D). Regional travel times through these revised 3-D velocity models have been computed using the Podvin/Lecomte finite difference algorithm and employed for purposes of model validation and the determination of Site-Specific Station Correction (SSSC) estimates for the IMS stations in this region. Validation studies of the DSS model have focused on comparisons with data from our Soviet explosion ground truth database, which currently consists of over 1000 carefully validated, regional P wave arrival time observations from distinct Soviet peaceful nuclear explosions (PNEs) and weapons tests. Results of these tests have confirmed that our tomographically refined DSS velocity model is highly accurate, with total root-mean-square (RMS) errors of less than 1 second for this dataset. In particular, we have demonstrated that this model predicts the observed ground truth travel times at locations near the IMS stations BRVK, NRI, TIK, YAK, PDY, TLY, ZAL, AAK and OBN with a degree of accuracy consistent with the regional seismic location goals of the project. For example, data recorded from a sample of 14 Soviet PNE events on a sparse network of 4-6 surrogate IMS stations were used to locate these explosions with and without the travel-time corrections predicted by our tomographically refined DSS 3-D velocity model, and it was found that the refined DSS model provides significantly more accurate seismic locations for these ground truth explosions than does the default IASPEI[1]-91 model (i.e. an average mislocation of 6.9 km as compared with 20.4 km). Similar validation studies of the tomographically refined WINPAK3D velocity model, conducted using ground truth earthquake data, have confirmed that this model is also quite accurate and that it provides significantly better seismic locations than other velocity models that have been proposed for this region. On the basis of these results, we have concluded that our current DSS and WINPAK3D velocity models are essentially final. P wave SSSC estimates, based on our revised velocity model of the Group 1 region, have now been estimated for all 30 Group 1 station locations; and we are in the process of delivering them to the Center for Monitoring Research for further independent evaluation. Finally, empirical correction surfaces that account for remaining unmodeled travel-time anomalies are also being estimated at a number of the Group 1 station locations using standard kriging algorithms. While these corrections appear to be quite precise, we are also investigating the potential utility of more sophisticated multi-station kriging algorithms that will satisfy seismic reciprocity constraints.

[1] International Association for Seismology and Physics of the Earth's Interior.

OBJECTIVES

The purpose of this effort is to develop improved 3-D velocity models, Site-Specific Station Corrections (SSSCs), and Slowness-Azimuth Station Corrections (SASCs) for eastern Asia, to demonstrate the effectiveness of these models and corrections in improving locations of seismic events, to evaluate the uncertainties associated with these improved models and corrections, and to install these models and corrections at the Center for Monitoring Research (CMR) and evaluate their performance. This calibration is focused on the 30 Group 1 IMS stations of eastern Asia shown in Figure 1. Our approach is based on a carefully crafted scientific approach, which effectively merges the limited observed calibration data with rigorous seismological and statistical modeling procedures. In our analysis the travel time for each station is represented as the sum of a model-based travel time and an empirical correction. The model-based component is obtained by raytracing through a 3-D velocity model of the crust and upper mantle regions surrounding each station, and the empirical correction is derived from calibration events observed at each IMS station where ground truth data are available.

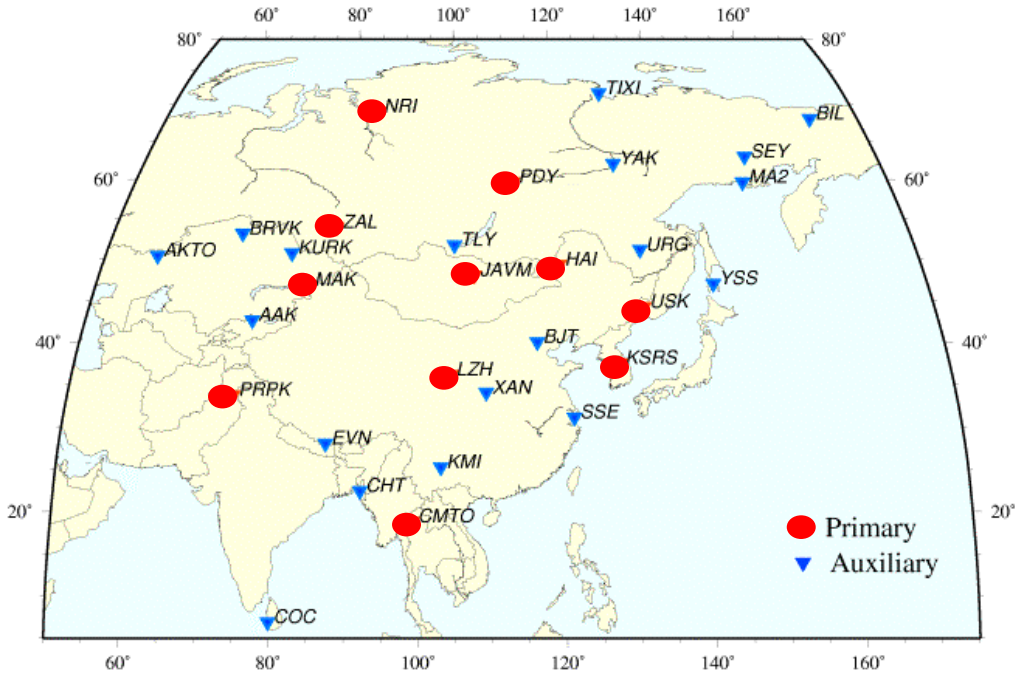

Figure 1. Locations of the 30 Group 1 IMS stations in eastern Asia.

RESEARCH ACCOMPLISHED

As noted above, we believe that a model-based approach to calculate travel-time corrections for Group 1 IMS stations in eastern Asia provides the best utilization of available knowledge for use in regions where the calibration data are sparse or non-existent, such as the many regions in Group 1, which are essentially aseismic. Therefore, the determination of travel-time tables and ultimately SSSCs is dependent on the identification of accurate velocity models to represent the crust and upper mantle in the regions surrounding each station. In defining these velocity models, we have drawn upon different knowledge bases depending on the levels of information available from the different areas and utilizing calibration data to update the model, in areas where the appropriate ground truth exists. The initial 3-D model (cf. Murphy *et al*, 2001) was composed of a hierarchy of models having different spatial resolutions; and this base model has continued to evolve during the past year, as more complete information has become available for different parts of the Group 1 region. Our general model for eastern Asia includes a new 1°-x-1° background model based on surface wave studies of Stevens *et al* (2001), a new China model developed at MIT by inverting travel-time data from Chinese earthquakes (see below), a new southeast Asia model compiled by Weston based on procedures similar to those used to define the WINPAK3D model, models for Thailand and the Korean peninsula based on surface wave studies modified by regional P-wave travel-time observations, and tomographically refined models covering much of the DSS and WINPAK3D areas where calibration event data were available.

One focus of the research efforts over the past year was to obtain a preliminary 3-D velocity model for China and the surrounding areas. To accomplish this objective, we have used the earthquake phase data from January 1990 to December 2001 from the Annual Bulletin of Chinese Earthquakes (cf. Chen, 1990-1998), which includes 16,642 earthquakes, recorded at 220 stations over 345,520 ray paths in China and surrounding areas (cf. Figure 2). These

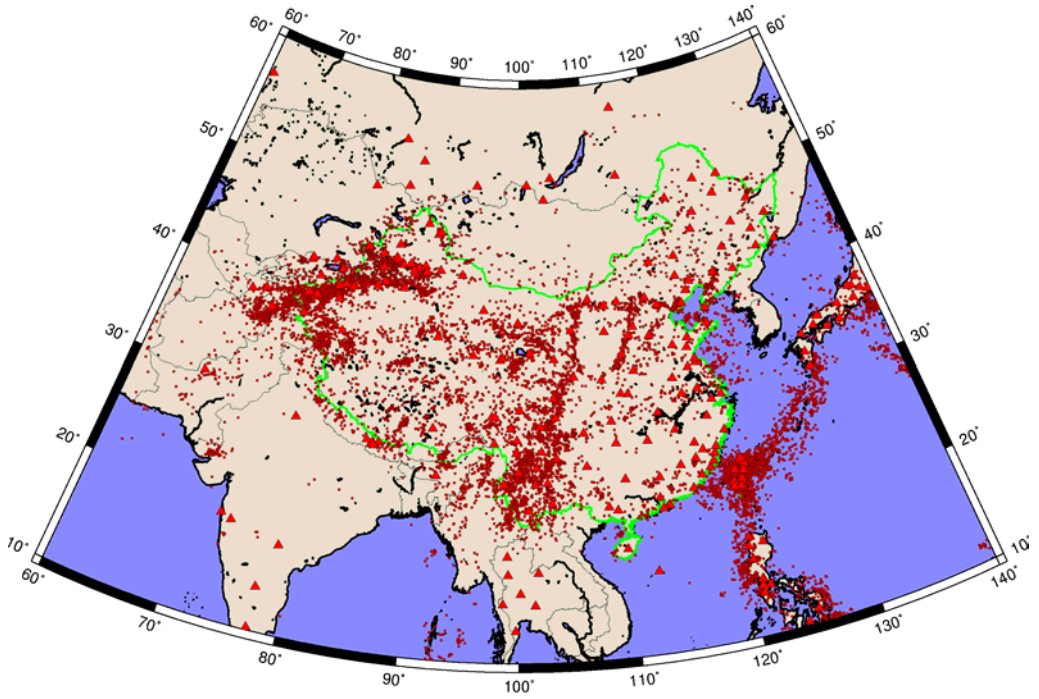

Figure 2. Locations of Chinese Bulletin events (circles) and stations (triangles) used to develop the velocity model for China.

data were analyzed by dividing the region into 1,312 1°-x-1° blocks covering China and Mongolia. In each block a 1-D velocity model was obtained by inverting the regional P-wave travel times over a 10°-x-10° region surrounding each block using a Monte Carlo algorithm to minimize the root-mean-square (RMS) travel-time residuals and invert for the optimal velocity models. Within each block the velocity structure is represented by a four-layer crust over one layer of upper mantle. The thickness of the top layer in each block was constrained to the values published by Laske *et al* (2001), and the Pn velocities were constrained to be within ± 0.1 km/sec of the values reported by Hearn and Ni (2001) for this region. The Monte Carlo inversion was then used to determine the thicknesses of the three other crustal layers, the four crustal P-wave velocities, and the Pn velocity in each block. The composite of the 1,312 1-D block models then gives the 3-D P-velocity model for the China/Mongolia region in the final model for eastern Asia. We illustrate the results of this model in Figure 3, showing the Pn velocity across the region.

Although there are some significant differences in detail, the Moho depths show the same general trends as reported in other models for the region (e.g. Laske *et al*, 2001; Stevens *et al*, 2001; Shapiro and Ritzwoller, 2001). There are some rather large differences in Pn velocities in specific areas from our model and those based on prior surface-wave inversion, and these will be investigated more closely. We have also compared the P-wave crustal velocity profiles as a function of depth for our model with the surface wave models and with those reported by other authors (viz. Mangino *et al*, 1999; Wu *et al*, 1997) at several specific locations within the China/Mongolia region and found that our P-wave velocity profiles fall nicely within the bounds of the other models in most areas.

It should be noted that the 3-D velocity model described above for China/Mongolia is viewed as preliminary and was not based on formal tomographic inversion of the available travel-time data; that remains to be done. However, we have made significant advances over the past year in tomographically refining the velocity models for two other areas (viz. the DSS region of the FSU and the WINPAK region of India/Pakistan) within our eastern Asia Group 1 study region. The state-of-the-art joint velocity tomography and event relocation algorithm, which we have

developed, uses the data set of regional seismic events to iteratively update the velocity model following a conjugate gradients technique that adjusts the velocity model to minimize the misfit between the calculated and observed

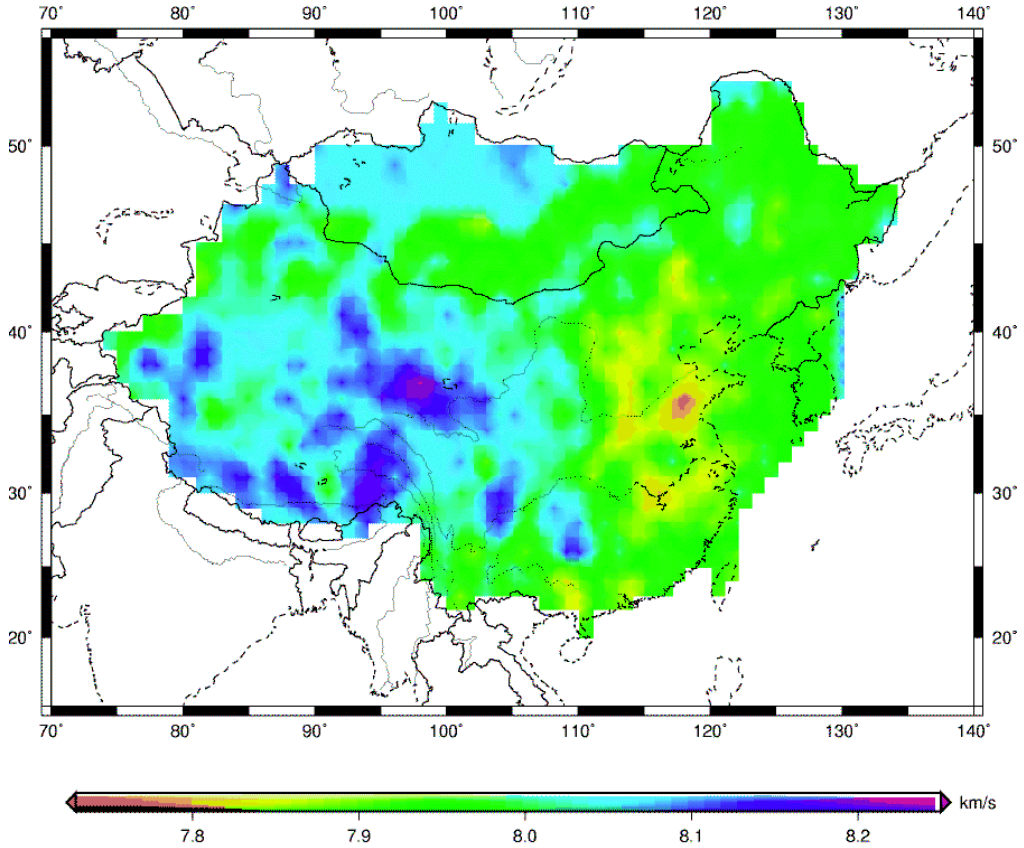

Figure 3. Pn upper mantle velocities for China/Mongolia derived from inversion of Chinese Bulletin earthquake data.

travel times from multiple stations and events, subject to smoothness constraints. The three major components of this algorithm are: (1) 3-D raytracing to predict first arrival times using a version of the Podvin/Lecomte (PL) method (cf. Podvin and Lecomte, 1991); (2) a 3-D grid search location algorithm to relocate events inside the appropriate velocity model; and (3) a linear conjugate gradient inversion algorithm to produce the updated velocity model inside each iteration of the process. Although we are currently only solving for Pn velocity in the inversion, model updates extend beyond Pn velocity. Based on the updated Pn velocity, velocities from the Moho down to 410 km are refined in a smooth manner, with a constant shift in velocity applied from the Moho extending to 210-km depth followed by a tapering between depths of 210 km and 410 km to provide a smooth transition to the 410-km discontinuity. This algorithm has been thoroughly tested and found to produce results that are reasonable and effective for adjusting velocity models to better represent the available calibration data. We have applied the tomography algorithm to two areas, where more abundant calibration data have been collected, using data from nuclear explosions at Semipalatinsk and Novaya Zemlya test sites and PNEs throughout the FSU, supplemented with some earthquake data, recorded at several current and historical stations in the DSS region and using data from a large sample of earthquakes in the WINPAK region recorded again at numerous regional stations. The results of these tomographic analyses are shown in Figure 4, where we have plotted the Pn velocities for the tomographically refined models covering the DSS and WINPAK3D areas. Focusing on the FSU region, there appears to be a definite correlation of the model results, derived from the tomography refinements, with published crust and upper mantle characteristics in the region. Examples are the two lower velocity features in the platform region to the north of BRVK which correlate remarkably well with regions of crustal thinning associated with the northeastern part of the Volga-Ural Uplift (northwest of BRVK) and with the crest of the West Siberian Platform (northeast of BRVK). The lower velocity region southeast of BRVK also correlates very well with the mapped northwestern part of the Kazakh foldbelt. So, the tomographic analyses produce velocity model refinements, which appear to be in reasonable agreement with geologic and tectonic features. Additional demonstration of the validity of these tomographic

refinements to the velocity models is provided by the resulting reduction in the travel-time residuals, as described below.

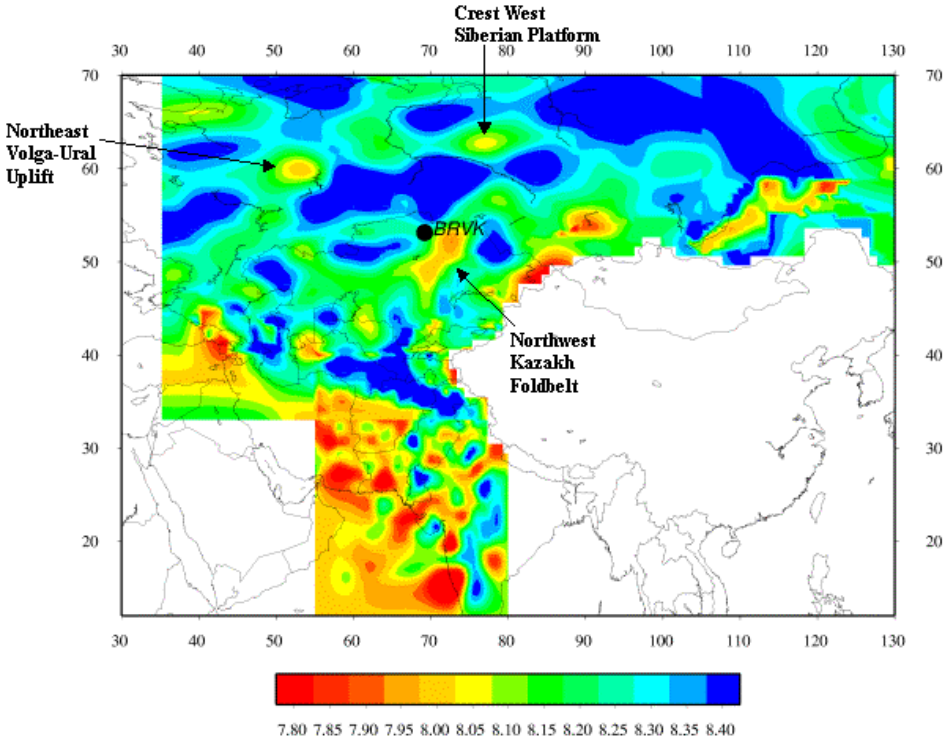

Figure 4. Tomographically refined Pn upper mantle velocities for the DSS and WINPAK regions.

We use a program module called QUILT to organize and assemble the models from the different regions covered by the Group 1 IMS stations into a composite 3-D model, which provides the basis for the SSSC calculations. The QUILT module allows us to integrate models with differing parameterizations and spatial resolutions from the different regions into a unified model that specifies the velocity profile at each geographic grid point as velocity/depth pairs from the earth's surface to a depth of 760 km, with velocity discontinuities at the ocean bottom, Moho, and the major mantle discontinuities at 410-km and 660-km depths. Grid spacing in the unified model is 0.5° in latitude, and longitude spacing is varied (with latitude) to be equal to latitude spacing, so as to preserve the grid aspect ratio. A second software module has been implemented to map the unified model from geographic to Cartesian coordinates that can be used by the Podvin/Lecomte raytracing algorithm and enable travel-time calculations at the resolution level required for the tomographic inversions and SSSC computations.

At the conclusion of the first year of this research program, we prepared estimates of the preliminary P-wave SSSCs for 20 Group 1 IMS stations, which were subsequently delivered to DTRA and CMR. As part of our program efforts over the past year, we have now computed the SSSCs for all 30 IMS station locations from the Group 1 region based on the revised velocity model described above. As an example we show in Figure 5 the P-wave surface-focus SSSCs for the area around station AAK. The values vary from –4.9 seconds to +7.0 seconds across the area. Largest negative values of the corrections occur on the far western and northern extremes, while greatest positive values occur to the southeast in China. Where the SSSCs are negative, the 3-D model travel times are shorter than those of IASPEI-91, indicating relatively higher velocities in the model; and, where the SSSCs are positive, they indicate model velocities are relatively lower than IASPEI-91. Digital versions of the SSSCs for surface focus plus 10 other focal depths (viz. 5, 10, 20, 30, 40, 50, 70, 100, 150, and 200 km) have been determined for each of the 30 Group 1 IMS station locations, and these have been delivered to the CMR for further testing and evaluation.

The ultimate test of the SSSCs derived from our 3-D velocity model is whether they enable more accurate event locations for the Group 1 region. To check this we made a number of P-wave travel-time comparisons for several individual IMS, or surrogate IMS stations, from our Group 1 region using explosion data from the FSU for ground

truth. As an example, Figure 6 shows observed P-wave travel-time residuals with respect to predictions based on the IASPEI-91 model and our refined 3-D velocity model for 55 Soviet PNEs observed at station BRVK. It is clear from the figure that the observed travel times are generally much faster than IASPEI-91 over most of the region. On the other hand, the size of the symbols is much smaller and more balanced, between positive and negative values,

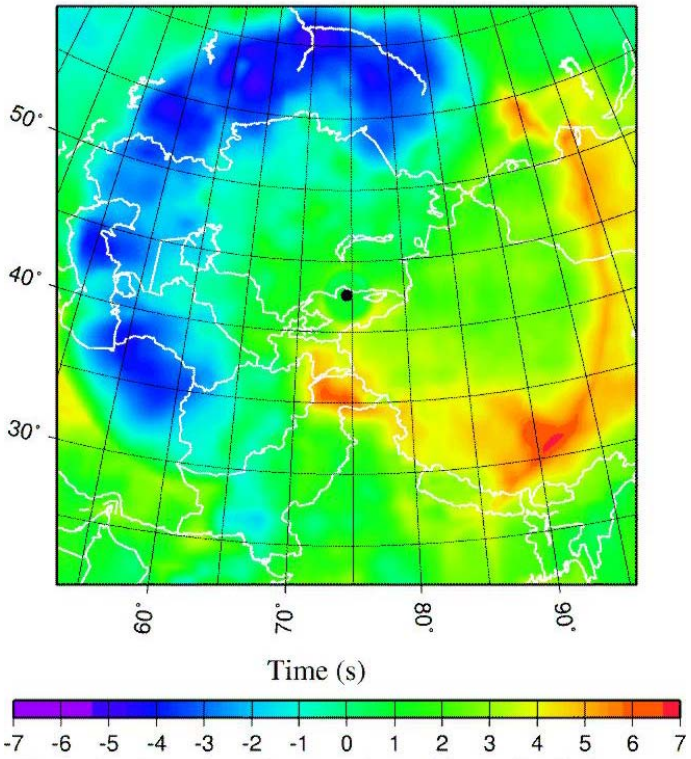

Figure 5. Surface-focus P-wave SSSCs for the region surrounding station AAK.

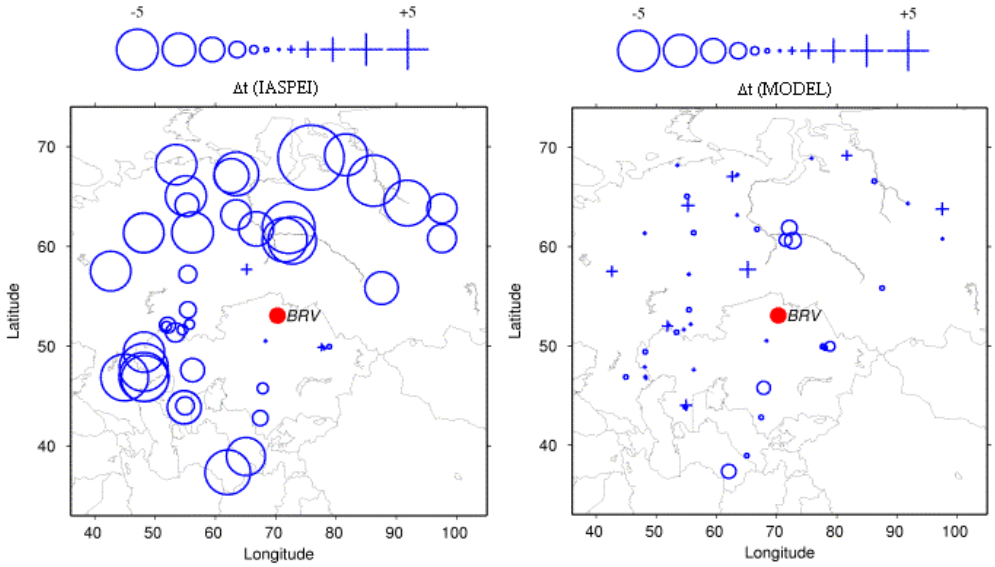

Figure 6. Comparison of observed BRVK P-wave residuals at calibration explosion locations for the IASPEI-91 model (left) and for our "final" 3-D velocity model (right).

for our 3-D velocity model. An even more dramatic example is shown in Figure 7 for station ELT. The large observed residuals for the PNEs with respect to the IASPEI-91 travel-time predictions are nearly completely accounted for in our final 3-D velocity model. There are significant reductions in both bias and scatter for the 3-D

model-based residuals over the IASPEI-91 results. Table 1 shows a more complete comparison between the IASPEI-91 and final 3-D velocity model for the average P-wave travel-time residuals for nine IMS or surrogate IMS stations from the Group 1 region determined from the PNE observations. It is noteworthy that at all stations, the

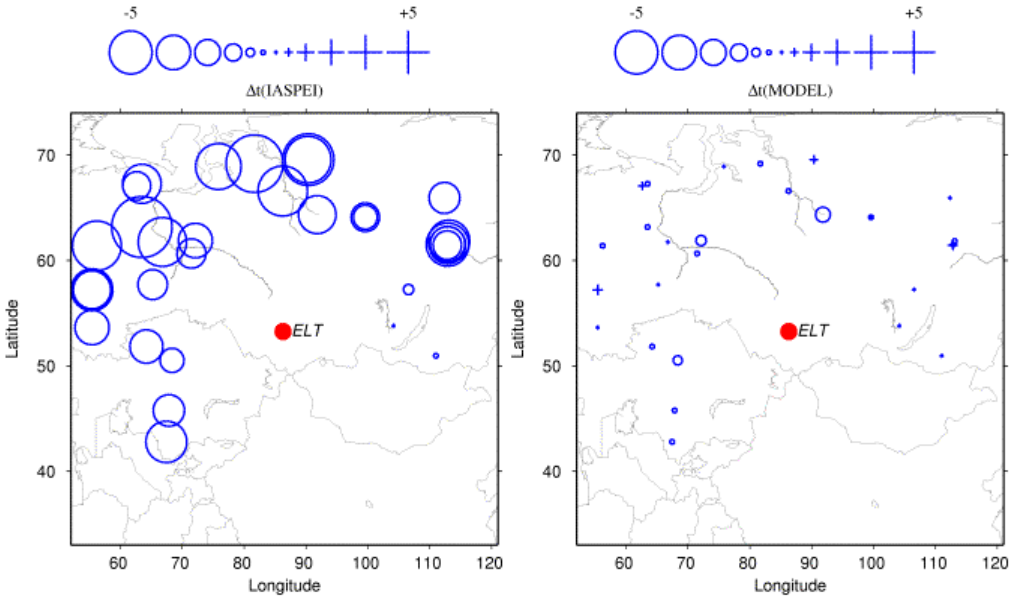

Figure 7. Comparison of observed ELT P-wave residuals at calibration explosion locations for IASPEI-91 model (left) and for our "final" 3-D velocity model (right).

Table 1. Summary of Soviet PNE statistics for IASPEI-91 and tomographically refined velocity model

	IASPEI-91		3-D Model	
Station	Δt, seconds	σ, seconds	Δt, seconds	σ, seconds
BRVK	-3.50	2.26	0.06	0.96
NRI	-3.34	2.93	-0.12	0.98
TIK	-4.33	1.38	0.27	0.90
YAK	-3.80	2.43	0.38	1.23
BOD (PDY)	-4.26	2.52	-0.56	0.93
IRK (TLY)	-3.46	2.67	-0.48	0.85
ELT (ZAL)	-4.10	1.66	-0.03	0.74
FRU (AAK)	-2.06	1.36	-0.07	1.14
M11 (OBN)	-4.01	1.83	-0.31	0.77

average travel-time residuals and their scatter are significantly reduced for our 3-D velocity model. As a further test, we used the data from 14 PNEs in the FSU, which were recorded at from four to six regional IMS or surrogate IMS stations. The events were relocated with our tomographically refined 3-D model as well as the IASPEI-91 model, and the locations were compared to the ground truth for the explosions. The mislocation measures are compared in Figure 8, where we see that the average error of 6.9 km for the 3-D model is much smaller than the average error of 20.4 km for the IASPEI-91 model.

By using calibration event data to enable tomographic refinement of the 3-D velocity model, we have designated a preference to account for travel-time residuals to the maximum extent possible as model adjustments, and then to estimate empirical station corrections to represent only any remaining unmodeled error. Kriging has been proposed as a method of representing the spatial dependence of empirical station corrections; and, to test this approach at selected stations, we have applied a simple kriging method to the travel-time residuals remaining after our

tomographic refinement of the 3-D velocity model of the DSS region. We applied the method to the stations with the most residual observations using primarily observations from PNEs in the FSU, except for station BRV where we had supplemental earthquake data. The derived empirical corrections, based on kriging, were found to further

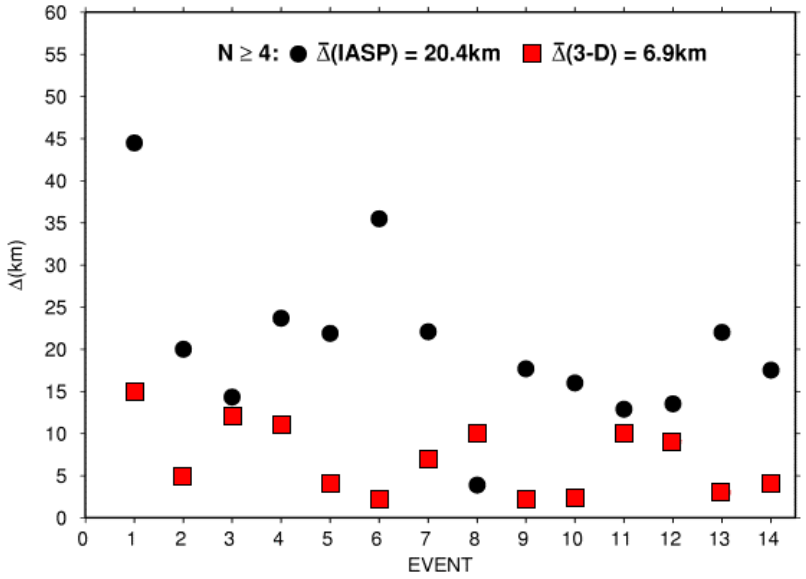

Figure 8. Comparison of regional seismic event location accuracies obtained for 14 selected Soviet PNE explosions with (3-D) and without (IASPEI) travel-time corrections predicted by the tomographically refined 3-D velocity model.

reduce the travel-time residual errors, as illustrated in Figure 9 for station BRVK. In this case the corrections were defined using the "leave one out" procedure, in which the correction surface was re-estimated for each explosion by leaving out the data point for that explosion. Application of the kriging correction further reduces the σ value from 0.92 seconds to 0.74 seconds, which we consider to be close to the lower bound on the resolution of the calibration process.

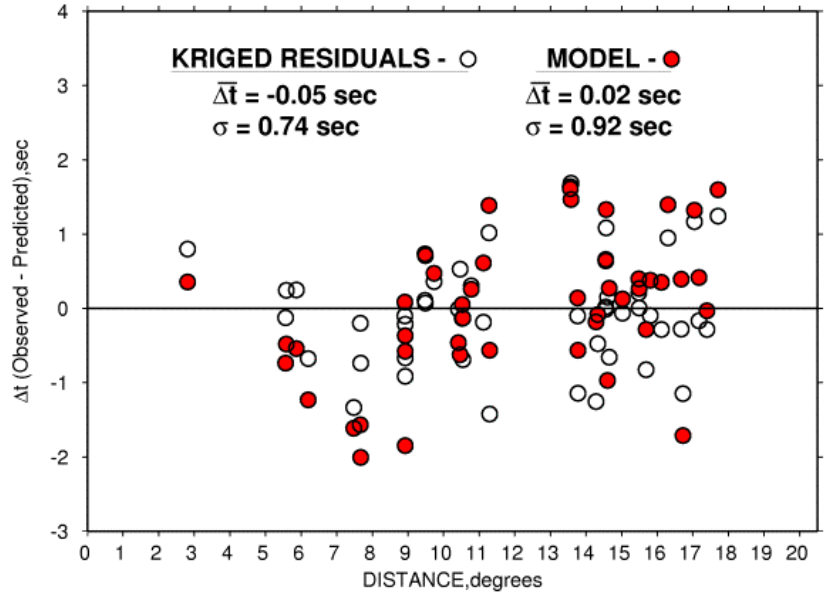

Figure 9. Comparison of PNE explosion travel-time residuals as a function of distance from station BRVK computed with respect to the kriged and to the refined 3-D velocity model.

Slowness and azimuth measurements are incorporated in routine locations at the IDC to improve location accuracy and decrease the size of error ellipses for small, poorly recorded events (Bondar *et al*, 1999). Azimuth and slowness estimates, however, can be biased, resulting in the need for SASCs. SASCs developed at the IDC are determined empirically using existing slowness and azimuth measurements at IMS stations; however, data at some IMS stations are insufficient to determine any corrections (Bondar *et al*, 1999). We have developed a preliminary technique to derive model-based SASCs that provide corrections at every point on a 3-D grid. This approach allows us to develop SASCs in regions where there are no previous data and for stations that have yet to be installed. Observed data can then be used to develop empirical corrections to the model-based SASCs.

Our technique for deriving SASCs is again based on the PL finite difference method, which we use for our travel-time calculations. Using reciprocity, travel times are calculated between a particular station location and all points in a 3-D grid of event locations. The slowness and azimuth observed at a station from a given event are the length and direction of the slowness vector defined by taking the gradient of travel time with respect to the station location. Our approach is to approximate this gradient by subtracting travel times computed for the actual station location from travel times calculated for perturbed station locations. Specifically, we compute travel times to each point in a 3-D grid, using the PL algorithm, from three different "station" locations: (1) at the proper station location, (2) displaced from the station by one node to the north, and (3) displaced from the station by one node to the east. We have chosen one-node displacement (5 km) for initial testing of this technique, but we are exploring varying the displacement amount for accuracy. The resulting travel-time grids are referred to as $T0_{ijk}$, $T1_{ijk}$ and $T2_{ijk}$, where $i, j,$ and k index the 3-D grid. The north and east components of the horizontal slowness vector that would be observed at the station from an event at node ijk are then determined by taking the derivative of the travel time with respect to the Podvin/Lecomte grid spacing (h) as follows:

$$p^N_{ijk} = (T1_{ijk} - T0_{ijk})/h \quad \text{and} \quad p^E_{ijk} = (T2_{ijk} - T0_{ijk})/h \qquad (1)$$

We convert to azimuth and scalar horizontal slowness by

$$\alpha_{ijk} = \arctan\,(p^E_{ijk} / p^N_{ijk}) \quad \text{and} \quad p_{ijk} = \sqrt{(p^N_{ijk})^2 + (p^E_{ijk})^2} \qquad (2)$$

where α_{ijk} is the azimuth and p_{ijk} is the horizontal slowness observed at the station from an event at node ijk. Azimuth is clockwise from north. Slowness is calculated in seconds/km and then converted to seconds/degree. Note that with this approach we obtain the slowness vector for each point in the 3-D grid. To determine SASCs at each node relative to the IASPEI-91 model (Kennett and Engdahl, 1991), we subtract slowness and azimuth values based on the IASPEI-91 model from those predicted for the 3-D model. Commonly, slowness-azimuth corrections are depicted as vectors in slowness space. With the model-based approach, this method of plotting is inappropriate because there would be a vector for every point on a fine grid. Therefore, we present our corrections as separate azimuth and scalar slowness maps. Figure 10 shows preliminary azimuth and slowness corrections for station BRVK relative to IASPEI-91. We will continue to extend and evaluate this SASC estimation capability.

CONCLUSIONS AND RECOMMENDATIONS

The results of this project to date demonstrate the value and effectiveness of our model-based approach to determine regional SSSCs for use in improving seismic event location. Our approach utilizes a fully 3-D velocity model, which we supplement with empirical corrections to take account of all the calibration data that are available for the region. We expect this approach to be more reliable for use in many areas, which are essentially aseismic, and to account for source depth dependence, which is beyond the capabilities of purely statistical approaches for most parts of the world. During the past year the 3-D velocity model, which forms the basis for our SSSC estimates, has been supplemented and revised to include new information from several parts of the Group 1 region as well as tomographic adjustments to some areas based on available calibration data. Calibration data have also been used to test and validate SSSC computational procedures and to demonstrate the effectiveness of the calibration corrections in improving locations and reducing uncertainties. We find that use of P-wave SSSCs derived from our 3-D velocity model for regional travel-time corrections can produce average σ uncertainty levels on the order of 1 second or less, which is better than nominal teleseismic uncertainty. Such corrections produce significant reductions in event location errors.

Over the remaining year of this project, there are a number of tasks that remain to be addressed. In addition to model refinements and supplementation of the database, we will be developing calibration corrections for alternative

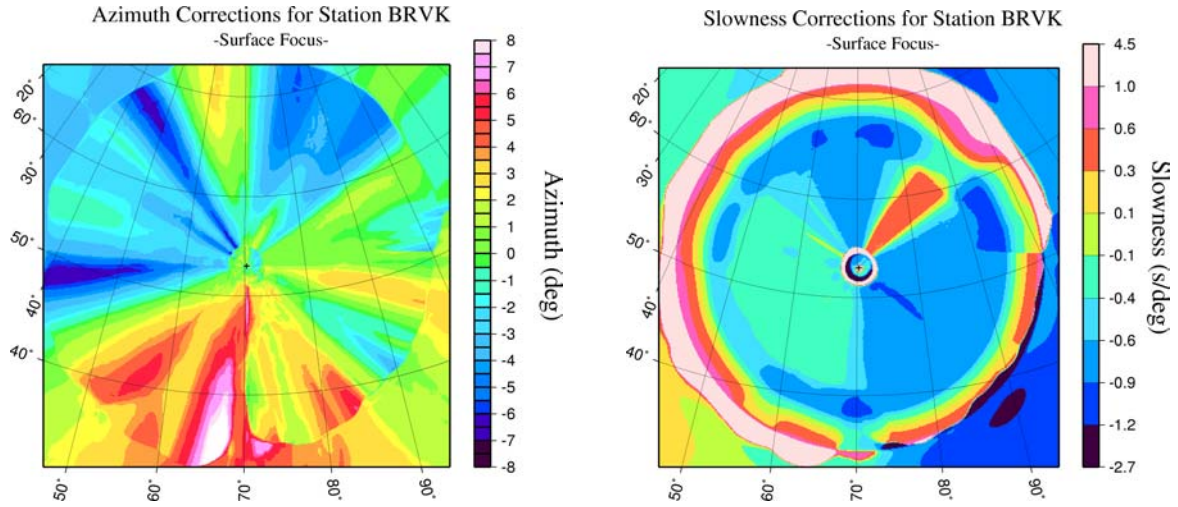

Figure 10. SASC corrections as derived from our 3-D tomographically updated model for station BRVK, relative to IASPEI-91, for a surface-focus source. Azimuth corrections are on the left. Scalar horizontal slowness corrections are in the figure to the right. Note that the color scale for slowness is not regularly spaced in order to better display the range of values.

regional phase types, refining procedures for predicting slowness-azimuth station corrections, and looking more closely at uncertainties and prediction errors. Specific areas of investigation include tomographic refinement and validation testing of China and other submodel areas, augmentation of the travel-time database for calibration events with other regional phases, including Pg, Sn, and Lg arrival times, improved empirical corrections to include improved kriging procedures which satisfy seismic reciprocity constraints, and estimation of prediction errors for the station corrections at the 30 Group 1 IMS station locations.

REFERENCES

Bondar, I., R. G. North, and G. Beall (1999), Teleseismic Slowness-Azimuth Station Corrections for the International Monitoring System Seismic Network, *Bull. Seism. Soc. Am.* **89**, 989-1003.

Chen, P. *et al* (1990-1998), *Annual Bulletin of Chinese Earthquakes* (ABCE), Chinese Seismology Bureau.

Hearn, T. M., and J. F. Ni (2001), Tomography and Location Problems in China Using Regional Travel-Time Data, *Proceedings of the 23rd Seismic Research Review: Worldwide Monitoring of Nuclear Explosions*, 155-160.

Kennett, B. L. N. and E. R. Engdahl (1991), Travel times for global earthquake location and phase identification, *Geophys. J. Int.* **105**, 429-465.

Laske, G., G. Masters, and C. Reif (2001), CRUST 2.0: A New Global Crustal Model at 2x2 Degrees, http://mahi.ucsd.edu/Gabi/rem.html.

Mangino, S., K. Priestley, and J. Ebel (1999), The Receiver Structure Beneath the China Digital Seismograph Network Stations, *Bull. Seism. Soc. Am.* **89**, 1053-1076.

Murphy, J., W. Rodi, M. Johnson, I. Kitov, D. Sultanov, B. Barker, C. Vincent, V. Ovtchinnikov, and Y Shchukin (2001), Seismic Calibration of Group 1 IMS Stations in Eastern Asia for Improved IDC Event Location, *Interim Technical Report* SAIC-01/1021, SAIC, San Diego, CA.

Podvin, P., and I. Lecomte (1991), Finite Difference Computation of Travel Times in Very Contrasted Velocity Models: A Massively Parallel Approach and Its Associated Tools, *Geophys. J. Int.* **105**, 271-284.

Shapiro, N. M., and M. H. Ritzwoller (2001), Monte-Carlo Inversion of Broadband Surface Wave Dispersion for a Global Shear Velocity Model of the Crust and Upper Mantle, *Geophys. J. Int.* **142**.

Stevens, J. L., D. A. Adams, and G. E. Baker (2001), Improved Surface Wave Detection and Measurement Using Phase-Matched Filtering with a Global One-Degree Dispersion Model, *Proceedings of the 23rd Seismic Research Review: Worldwide Monitoring of Nuclear Explosions*, 420-430.

Wu, F. T., A. L. Levshin, and V. M. Kozhevnikov (1997), Rayleigh Wave Group Velocity Tomography of Siberia, China and Vicinity, *Pure Appl. Geophys.* **149**, 447-473.